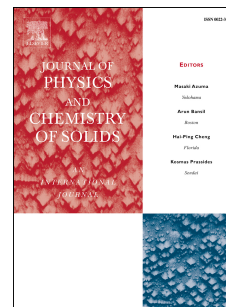


# Journal Pre-proof

Encapsulating palladium nanoparticles inside ethylenediamine functionalized and crosslinked chlorinated poly(vinyl chloride) nanofibers as an efficient and stable heterogeneous catalyst for coupling reactions

Min Qin, Qingqing Wang, Yijun Du, Linjun Shao, Chenze Qi, Hongyu Tao



PII: S0022-3697(20)30844-1

DOI: <https://doi.org/10.1016/j.jpcs.2020.109674>

Reference: PCS 109674

To appear in: *Journal of Physics and Chemistry of Solids*

Received Date: 2 April 2020

Revised Date: 27 June 2020

Accepted Date: 21 July 2020

Please cite this article as: M. Qin, Q. Wang, Y. Du, L. Shao, C. Qi, H. Tao, Encapsulating palladium nanoparticles inside ethylenediamine functionalized and crosslinked chlorinated poly(vinyl chloride) nanofibers as an efficient and stable heterogeneous catalyst for coupling reactions, *Journal of Physics and Chemistry of Solids* (2020), doi: <https://doi.org/10.1016/j.jpcs.2020.109674>.

This is a PDF file of an article that has undergone enhancements after acceptance, such as the addition of a cover page and metadata, and formatting for readability, but it is not yet the definitive version of record. This version will undergo additional copyediting, typesetting and review before it is published in its final form, but we are providing this version to give early visibility of the article. Please note that, during the production process, errors may be discovered which could affect the content, and all legal disclaimers that apply to the journal pertain.

© 2020 Published by Elsevier Ltd.

## **Author statement**

Min Qin: Preparation and characterization of Pd@ACPVC catalyst

Qingqing Wang: Evaluation of catalytic performance of Pd@ACPVC catalyst

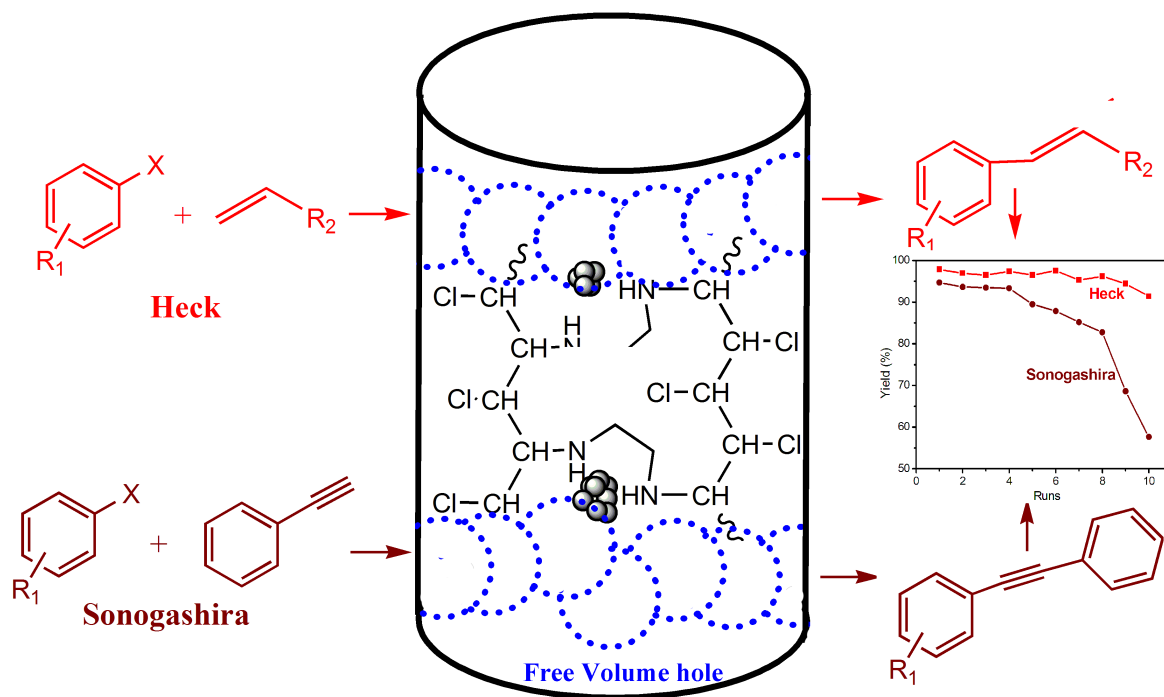
Yijun Du: Supervision

Linjun Shao: data analysis, writing-original draft preparation.

Chenze Qi: Characterization

Hongyu Tao: data analysis

Journal Pre-proof



Journal Pre-proof

Encapsulating palladium nanoparticles inside ethylenediamine functionalized and crosslinked chlorinated poly(vinyl chloride) nanofibers as an efficient and stable heterogeneous catalyst for coupling reactions

Min Qin, Qingqing Wang, Yijun Du<sup>\*</sup>, Linjun Shao<sup>\*</sup>, Chenze Qi, Hongyu Tao

*Zhejiang Key Laboratory of Alternative Technologies for Fine Chemicals Process, Shaoxing University, Zhejiang 312000, China*

<sup>\*</sup>Address correspondence to Linjun Shao (shaolinjun@usx.edu.cn)

**Abstract**

Palladium chloride and chlorinated poly(vinyl chloride) (CPVC) mixture were prepared into homogeneous solution, followed by electrospinning to make uniform nanofibers with average diameter of ~460 nm. Then, these composite nanofibers were treated in ethylenediamine solution to functionalize and crosslink the CPVC molecules inside the nanofibers to improve their chelating ability and solvent resistance. The functionalization and crosslinking of CPVC molecules inside composite nanofibers were confirmed by SEM, FT-IR, EA and PALS characterizations. The catalytic performance of these palladium encapsulated CPVC nanofibers (Pd@ACPVC) have been evaluated by the Heck and Sonogashira reactions. The catalysis results demonstrate that this Pd@ACPVC catalyst was very effective and stable to catalyze the coupling reaction of aromatic iodides with alkenes (Heck reaction) or phenyl acetylene (Sonogashira reaction) to afford the coupling products in moderate to excellent yields. Due to the regular fibrous structure, the Pd@ACPVC could be readily separated and recovered from reaction mixture. In addition, the Pd@ACPVC could be separately reused for 10 times for Heck reaction and 8 times for Sonogashira reaction without significant decrement of coupling yields. After careful investigation, the palladium leaching from Pd@ACPVC in the reuse procedure could be ascribed to the loss of chelating groups (amino groups) and expansion of free volume holes in the composite nanofibers. The excellent catalytic activity and stability of Pd@ACPVC could be attributed to the strong chelating ability of amino groups, encapsulation of palladium nanoparticles and ultrafine fiber.

**Keywords:** Palladium nanoparticles; chlorinated poly(vinyl chloride) nanofibers; electrospinning; coupling reaction; free volume.

## 1. Introduction

Palladium catalysts have attracted much attention for their high catalytic performance in organic reactions, which have been widely applied in chemical industry and academic researches for many carbon-carbon bond transformations [1,2]. Homogeneous palladium catalysts are highly active and selective to catalyze the reactions, but suffer the problems of high cost, toxicity and difficulties in separation and recovery [3]. Hence, much effort has been devoted to developing heterogeneous palladium catalysts for easy recovery and reuse [3-9]. However, it is still a great challenge to mitigate the leaching of palladium species from the heterogeneous catalysts in catalysis procedure. Therefore, exploiting facile methods to prepare highly active and stable heterogeneous palladium catalysts is still in great demand.

In order to retain palladium activity and simplify preparation procedure, palladium species are generally deposited on the surface of solid matrices with larger specific surface area [10-12]. However, destruction of solid matrices, severe reaction conditions (e.g. high reaction temperature) and polar solvent would weaken the bond strength between solid matrices with palladium species [13,14], resulting in the aggregation and leaching of palladium nanoparticles in catalysis. Thus, although the synthesis of ultrafine palladium nanoparticles on solid matrices has been achieved by using ligands and capping agents [15,16], the inhibition of palladium aggregation and leaching in catalysis procedure was still a great challenge. As the capping agents can promote the formation of ultrafine palladium nanoparticles, we have speculated that the stability of palladium nanoparticles could be improved by encapsulating them inside the solid polymer matrices due to the capping effect from the polymer chains. Moreover, the catalytic activity of these encapsulated palladium nanoparticles could be retained provided the reactant molecules could freely access the catalytic sites [17-19].

Electrospinning is a versatile method to fabricate polymer ultrafine fibers directly from polymer solutions or melts. The larger specific surface area of these fibers makes them hold great potential in catalysis. The polymer nanofibers are ideal solid matrices to encapsulate the palladium nanoparticles for their ultrafine fiber, which facilitates the diffusion of reactants and products inside the nanofibers [20-22]. Moreover, compared with the particulate solid matrices, the nanofiber structure not only can make the fibers achieve a relatively larger specific area, but also can be readily separated and recovered from the reaction mixture by simple filtration [23,24].

Till now, various inorganic and organic materials have been used as solid matrices to support palladium catalyst [25]. Chlorinated poly(vinyl chloride) (CPVC) and poly(vinyl chloride) (PVC) have been used as the supporting matrices for its low cost, excellent mechanical property and easy modification [26-29]. In our previous studies [30,31], CPVC has been electrospun into nanofibers for the deposition of palladium nanoparticles. The CPVC was readily electrospun into well-defined nanofibers, but these CPVC nanofibers were easily dissolved in many organic solvents (e.g. chloroform, tetrahydrofuran and *N,N*-dimethylformamide). Therefore, crosslinking of CPVC molecules were essential to improve the solvent resistance of CPVC nanofibers. Herein, ethylenediamine was used to crosslink and functionalize the CPVC molecules inside the palladium encapsulated CPVC composite nanofibers. The stability of palladium nanoparticles would be improved by the chelating ability of amino groups and capping effect of crosslinked CPVC molecules (Scheme 1). The catalytic performance of these palladium encapsulated CPVC composite nanofibers (Pd@ACPVC) was evaluated by Heck and Sonogashira reactions.

## 2. Experimental section

### 2.1. Materials

Chlorinated polyvinyl chloride (CPVC, Average molecular weight: 85000) was bought from Hangzhou Qianjing Chemical Co., Ltd (Zhejiang, China). Ethylenediamine and the reagents for Heck and Sonogashira reactions (Analytical grade) were purchased from Aladdin Chemical Co. Ltd (Shanghai, China). Palladium chloride ( $\text{PdCl}_2$ ) (Chemical grade) was bought from Hangzhou Changqing Chemical Industrial Co., Ltd (Zhejiang, China). All the reagents were directly used as received without further purification.

### 2.2. Preparation of palladium doped CPVC nanofiber via electrospinning

CPVC powder (2.0 g),  $\text{PdCl}_2$  (50 mg) and NaCl (50 mg) were put into a flask containing 6.3 mL tetrahydrofuran (THF) and 12.0 mL *N,N*-dimethylformamide (DMF). The mixture was stirred magnetically for 12 hours to afford red homogeneous solution. Then, the solution was transferred into an electrospinning equipment to make palladium encapsulated CPVC nanofibers (FM1206, Beijing Future Material Sci-tech Co., Ltd, China). The electrospinning parameters were as follows: needle gauge: 21 G; feeding rate: 0.08 mL/h; applied voltage: 25 kV, work distance: 25 cm. The resultant nanofiber mat (Pd@CPVC) was dried under vacuum at 80 °C to remove the residual solvent.

### 2.3. Crosslinking of CPVC molecules inside the nanofibers

The Pd@CPVC fiber mat (0.2 g) was added into a flask containing 4.5 mL ethylenediamine and 12.7 mL ethanol. After reacting at 60 °C for 12 hours, the fiber mat was filtrated and washed three times by water. The fiber mat was dried under vacuum at 80 °C for 12 hours and signed as Pd@ACPVC.

#### 2.4. Reduction of Pd<sup>2+</sup> cations into Pd<sup>0</sup> nanoparticles

The Pd@ACPVC was immersed in 12.7 mL ethanol solution containing 1.0 g NaBH<sub>4</sub>. After stirring for 5.0 hours, the Pd@ACPVC was recovered by filtration and dried under reduced pressure at 25 °C for 12 hours. The palladium content in the Pd@ACPVC was 0.94 wt.%, which was determined by inductively coupled plasma-atomic emission spectroscopy (ICP-AES).

For comparison, CPVC nanofibers were also prepared by the same method as that of Pd@CPVC but without the addition of PdCl<sub>2</sub> and NaCl. Then, the CPVC nanofibers were reacted with ethylenediamine by the identical procedure as that of Pd@ACPVC to synthesize aminated and crosslinked CPVC nanofibers (ACPVC).

#### 2.5. Typical procedure for Heck reaction

Aromatic iodide (1.0 mmol), alkene (2.0 mmol), triethylamine (2.5 mmol) and glycol (0.2 g) were added into a tubular reactor containing 25 mg Pd@ACPVC fiber mat (Pd content: 2.21 μmol) and 3.2 mL *N,N*-dimethylacetamide (DMAc). The reaction mixture was carried out with magnetically stirring at 110 °C. The reaction progress was monitored by thin layer chromatography (TLC) and gas chromatograph/mass spectrometer (GC/MS). After reaction, 10 mL water was added into the reaction mixture to quench the reaction and then the reaction mixture was extracted with ethyl acetate (3 × 10 mL). Solvent of extracted solution was removed under reduced pressure to afford the crude product, which was further purified by silica gel chromatography. The coupling products were confirmed by <sup>1</sup>H NMR spectra and mass spectra.

The Pd@ACPVC catalyst was recovered by filtration and then washed by DMAc and water. Then, the Pd@ACPVC catalyst was dried at 80 °C under reduced pressure for reuse. The reuse procedure is the same as that of Pd@ACPVC catalyzed Heck reaction.

Characterization data of Heck reaction products was shown as follows:

Butyl cinnamate:  $^1\text{H}$  NMR (400 MHz,  $\text{CDCl}_3$ )  $\delta$  7.62 (d,  $J = 16.0$  Hz, 1H), 7.50 – 7.42 (m, 2H), 7.36 – 7.29 (m, 3H), 6.38 (d,  $J = 16.0$  Hz, 1H), 4.20 – 4.11 (m, 2H), 1.63 (dt,  $J = 14.6, 6.8$  Hz, 2H), 1.45 – 1.29 (m, 2H), 0.91 (t,  $J = 7.4$  Hz, 3H). MS  $m/z$  (%): 204 (23.5), 148 (71.5), 147 (59.2), 131 (99.9), 103 (13.3), 77(22.5).

(*E*)-butyl 3-(2-fluorophenyl)acrylate:  $^1\text{H}$  NMR (400 MHz,  $\text{CDCl}_3$ )  $\delta$  7.81 (d,  $J = 16.2$  Hz, 1H), 7.54 (td,  $J = 7.6, 1.5$  Hz, 1H), 7.35 (ddd,  $J = 15.3, 5.3, 1.7$  Hz, 1H), 7.20 – 7.06 (m, 2H), 6.54 (d,  $J = 16.2$  Hz, 1H), 4.22 (t,  $J = 6.7$  Hz, 2H), 1.70 (dt,  $J = 14.6, 6.8$  Hz, 2H), 1.53 – 1.35 (m, 2H), 0.97 (t,  $J = 7.4$  Hz, 3H). MS  $m/z$  (%): 222 (14.2), 167 (14.1), 166 (41.0), 149 (99.9), 146 (23.2), 121 (34.3), 101 (48.9), 75 (14.3).

(*E*)-butyl 3-(4-fluorophenyl)acrylate:  $^1\text{H}$  NMR (400 MHz,  $\text{CDCl}_3$ )  $\delta$  7.64 (d,  $J = 16.0$  Hz, 1H), 7.56 – 7.47 (m, 2H), 7.12 – 7.03 (m, 2H), 6.36 (d,  $J = 16.0$  Hz, 1H), 4.21 (t,  $J = 6.7$  Hz, 2H), 1.69 (dt,  $J = 14.6, 6.8$  Hz, 2H), 1.51 – 1.36 (m, 2H), 0.97 (t,  $J = 7.4$  Hz, 3H). MS  $m/z$  (%): 222 (19.7), 165 (27.8), 166 (93.0), 149 (99.9), 121 (35.4), 101 (35.17).

(*E*)-butyl 3-(2-bromophenyl)acrylate:  $^1\text{H}$  NMR (400 MHz,  $\text{CDCl}_3$ ) 8.05 (d,  $J = 15.9$  Hz, 1H), 7.61 (d,  $J = 8.0$  Hz, 2H), 7.32 (s, 1H), 7.29 – 7.19 (m, 1H), 6.39 (d,  $J = 15.9$  Hz, 1H), 4.23 (t,  $J = 6.7$  Hz, 2H), 1.75 – 1.66 (m, 2H), 1.45 (dd,  $J = 15.0, 7.5$  Hz, 2H), 0.97 (t,  $J = 7.4$  Hz, 3H). MS  $m/z$  (%): 282 (5.2), 209 (169), 211 (162), 147 (99.9), 102 (28), 1101 (10.2)

(*E*)-butyl 3-(4-chlorophenyl)acrylate:  $^1\text{H}$  NMR (400 MHz,  $\text{CDCl}_3$ )  $\delta$  7.63 (d,  $J = 16.0$  Hz, 1H), 7.46 (d,  $J = 8.5$  Hz, 2H), 7.36 (d,  $J = 8.5$  Hz, 2H), 6.42 (d,  $J = 16.0$  Hz, 1H), 4.21 (t,  $J = 6.7$  Hz, 2H), 1.69 (dt,  $J = 14.6, 6.8$  Hz, 2H), 1.44 (dd,  $J = 15.1, 7.5$  Hz, 2H), 0.96 (dd,  $J = 13.8, 6.4$  Hz, 3H). MS  $m/z$  (%) 238 (21.6), 182 (99.9), 165 (88.6), 137 (27.9), 102 (37.6), 75 (25.3).

(*E*)-butyl 3-*o*-tolylacrylate:  $^1\text{H}$  NMR (400 MHz,  $\text{CDCl}_3$ )  $\delta$  7.97 (d,  $J = 15.9$  Hz, 1H), 7.59 – 7.51 (m, 1H), 7.31 – 7.16 (m, 3H), 6.36 (d,  $J = 15.9$  Hz, 1H), 4.21 (t,  $J = 6.7$  Hz, 2H), 2.44 (s, 3H), 1.76 – 1.63 (m, 2H), 1.51 – 1.38 (m, 2H), 0.97 (t,  $J = 7.4$  Hz, 3H). MS  $m/z$  (%): 218 (24.2), 147 (30.5), 146 (12.2), 145 (99.9), 116(73.6), 115(64.8), 117 (47.3), 91 (21.8).

(*E*)-butyl 3-*m*-tolylacrylate:  $^1\text{H}$  NMR (400 MHz,  $\text{CDCl}_3$ )  $\delta$  7.65 (d,  $J = 16.0$  Hz, 1H), 7.36 – 7.15 (m, 4H), 6.43 (d,  $J = 16.0$  Hz, 1H), 4.20 (t,  $J = 6.7$  Hz, 2H), 2.36 (d,  $J = 5.2$  Hz, 3H), 1.75 – 1.62 (m, 2H), 1.44 (dd,  $J = 15.0, 7.5$  Hz, 2H), 0.96 (t,  $J = 7.4$  Hz, 3H). MS  $m/z$  (%): 218 (30.0), 162 (69.2), 147 (44.7), 145 (99.9), 117 (27.7), 116 (15.1), 115 (53.8), 91 (25.5).

(*E*)-butyl 3-*p*-tolylacrylate:  $^1\text{H}$  NMR (400 MHz,  $\text{CDCl}_3$ )  $\delta$  7.63 (d,  $J = 16.0$  Hz, 1H), 7.54 – 7.39 (m, 2H), 6.96 – 6.81 (m, 2H), 6.31 (d,  $J = 16.0$  Hz, 1H), 4.19 (t,  $J = 6.7$  Hz, 2H), 3.82 (d,  $J = 8.0$  Hz, 3H), 1.74 – 1.61 (m, 2H), 1.51 – 1.35 (m, 2H), 1.00 – 0.65 (m, 3H). MS  $m/z$  (%): 218 (34.9), 162 (95.6), 161 (26.17), 147 (22.3), 145 (99.9), 115 (46.5), 117 (28.8).

Methyl cinnamate:  $^1\text{H}$  NMR (400 MHz,  $\text{CDCl}_3$ )  $\delta$  7.70 (d,  $J = 16.0$  Hz, 1H), 7.53 (dd,  $J = 6.5, 2.9$  Hz, 2H), 7.46 – 7.29 (m, 3H), 6.45 (d,  $J = 16.0$  Hz, 1H), 3.81 (s, 3H). MS  $m/z$  (%): 162 (55.0), 161 (27.0), 132 (10.1), 131 (99.9), 103 (59.8), 102 (15.4), 77 (32.2).

(*E*)-1,2-diphenylethene:  $^1\text{H}$  NMR (400 MHz,  $\text{CDCl}_3$ )  $\delta$  7.53 (d,  $J = 7.5$  Hz, 4H), 7.37 (t,  $J = 7.6$  Hz, 4H), 7.26 (d,  $J = 3.7$  Hz, 2H), 7.12 (s, 2H). MS (EI)  $m/z$  (%): 180 (99.9), 179 (57.8), 178 (336), 165 (23.6), 89 (15.6)

(*E*)-butyl 3-(4-nitrophenyl)acrylate:  $^1\text{H}$  NMR (400 MHz,  $\text{CDCl}_3$ )  $\delta$  7.62 (d,  $J = 16.0$  Hz, 1H), 7.49 – 7.41 (m, 2H), 7.35 (dd,  $J = 8.7, 2.0$  Hz, 2H), 6.41 (d,  $J = 16.0$  Hz, 1H), 4.21 (t,  $J = 6.7$  Hz, 2H), 1.69 (dt,  $J = 14.6, 6.8$  Hz, 2H), 1.51 – 1.36 (m, 2H), 0.96 (t,  $J = 7.4$  Hz, 3H). MS  $m/z$  (%): 239 (11.2), 194 (54.5), 193 (43.7), 176 (99.9), 177 (19.2), 102 (38.1), 56 (33.4), 130 (31.6).

## 2.6. Typical procedure for Sonogashira reaction

Aromatic iodide (1.0 mmol), alkyne (2.0 mmol),  $K_2CO_3$  (3.0 mmol), glycol (0.2 g) and CuI (0.02 mmol) were added into a tubular reactor containing 15 mg Pd@CPVC fiber mat and 3.2 mL DMAc. The reaction was carried out at 110 °C with magnetic stirring. The post treatment was the same as that of Pd@CPVC catalyzed Heck reaction. The coupling products were confirmed by the  $^1H$  NMR spectra and mass spectra.

Characterization data of Sonogashira reaction products was shown as follows:

1,2-Diphenylethyne:  $^1H$  NMR (400 MHz,  $CDCl_3$ )  $\delta$  7.55-7.59 (m, 3H), 7.42-7.44 (m, 1H), 7.35-7.37 (m, 3H), 7.27-7.29 (m, 1H), 7.22-7.25 (m, 1H); MS m/z (%) 178 (99.9), 176 (20.5), 179 (15.2), 177 (11.3), 152 (11.2), 151 (8.6), 76 (7.6), 89(6.4), 150(5.7), 126(5.1).

1-Fluoro-4-(2-phenylethynyl)benzene:  $^1H$  NMR (400 MHz,  $CDCl_3$ )  $\delta$  7.26-7.30 (m, 2H), 7.43-7.45 (m, 3H), 7.48-7.51(m, 1H), 7.54-7.57(m, 1H), 7.60-7.64(m, 2H). MS m/z (%) 196 (99.9), 197 (15.5), 194 (13.3), 170 (9.0), 98 (8.0), 175 (7.5), 195 (6.8), 85 (5.2), 169 (4.4), 144 (4.0).

1-Bromo-2-(2-phenylethynyl)benzene:  $^1H$  NMR (400 MHz,  $CDCl_3$ )  $\delta$  7.57 – 7.49 (m, 4H), 7.41 – 7.29 (m, 6H). MS m/z (%) 258 (96.0), 256 (99.9), 176 (69.5), 151 (17.6), 88 (18.6).

1-Chloro-2-(2-phenylethynyl)benzene:  $^1H$  NMR (400 MHz,  $CDCl_3$ )  $\delta$  7.58-7.61(m, 4H), 7.46-7.78(m, 6H). MS m/z (%) 212 (99.9), 176 (37.0), 151 (13.0).

1-Methyl-2-(2-phenylethynyl)benzene:  $^1H$  NMR (400 MHz,  $CDCl_3$ )  $\delta$  7.56-7.58(m, 2H), 7.51(d, 1H, J=7.6 Hz), 7.43-7.46 (m, 3H), 7.33(d, 2H, J=3.0 Hz), 7.22-7.26(m, 1H), 2.47(s, 3H). MS m/z (%) 192 (99.9), 191 (96.1), 189 (36.1), 165 (26.2), 190 (18.7), 193 (15.1), 115 (11.5), 95 (7.0), 163 (5.5), 164 (4.8).

1-Methyl-4-(2-phenylethynyl)benzene:  $^1\text{H}$  NMR (400 MHz,  $\text{CDCl}_3$ )  $\delta$  6.96-7.00(m, 4H), 7.12-7.15 (m, 2H), 7.15-7.17(m, 2H), 7.25 (m, 1H), 2.31(s, 3H). MS  $m/z$  (%) 192 (99.9), 191 (49.0), 189 (25.0), 193 (15.9), 165 (15.5), 190 (12.3), 115 (5.3), 95 (4.7), 139 (4.0), 163 (3.9).

2-(2-Phenylethynyl)thiophene:  $^1\text{H}$  NMR (400 MHz,  $\text{CDCl}_3$ )  $\delta$  7.50 (dd,  $J = 4.9, 1.6$  Hz, 2H), 7.32 (dd,  $J = 5.0, 1.7$  Hz, 3H), 7.29 – 7.24 (m, 2H), 6.99 (dd,  $J = 5.1, 3.7$  Hz, 1H). MS  $m/z$  (%) 184 (99.9), 152 (17.5), 139 (22.3).

## 2.7. Instrumentation

The fiber surface morphologies were recorded by scanning electron microscopy (SEM) (Jeol, Jsm-6360lv, Tokyo, Japan). Nanofiber diameters were determined from their corresponding SEM images. For each sample, at least fifty nanofibers were counted for the determination of mean diameter. Surface mapping was done on an energy dispersive X-ray spectroscopy (Oxford EDX system) (SEM-EDS) (X-act, Oxford, Britain). The chemical structures of the fiber mats were analyzed by Fourier transform infrared spectroscopy (FT-IR) with the accessory of attenuated total reflection (Nicolet, Nexus-470, Wisconsin, USA). Thermal stability of the fiber mats in atmospheric air was performed on a thermogravimetric analyzer (TGA) (Beijing Scientific Instrument Factory, Beijing, China) with heating rate of  $10\text{ }^\circ\text{C}/\text{min}$ . The palladium dispersion in Pd@ACPVC was analyzed by X-ray diffraction (XRD) (Empyrean, PANalytical, Almelo, Netherlands). The electronic states of palladium were determined by X-ray photoelectron spectroscopy (Escalab250Xi, Thermo Fisher Scientific, USA).  $\text{C}_{1s}$  of 284.6 eV was used as the internal reference for calibration.

Positron annihilation lifetime spectroscopic (PALS) measurements were done using a fast-fast lifetime spectrometer (EG&G ORTEC Co., Tennessee, USA) at room temperature.

Time resolution was 190 ps at a  $^{60}\text{Co}$  prompt peak of 1.18 MeV and 1.33 MeV. A  $^{22}\text{Na}$  positron source ( $6.0 \times 10^5$  Bq) on 3  $\mu\text{m}$  thick Kapton films was sandwiched within two identical fiber mats. Analysis of positron lifetime spectrum was performed using a three-component fitting LT 9.0 program.

The fiber mat (~10 mg) was first dissolved in a mixture of fuming nitric acid and 98% sulfuric acid (v/v: 1/3) and then diluted to 50 mL with deionized water. The palladium concentration was measured by inductively coupled plasma-atomic emission spectroscopy (ICP) (Leeman ICP-AES Prodigy XP, New Hampshire, USA).

The quantitative analysis of the coupling products was performed on an Agilent GC/MS instrument (Agilent, GC6890/5975 MSD, California, USA). The coupling products were dissolved in  $\text{CDCl}_3$  solution and characterized by  $^1\text{H}$  NMR spectra (AVANCE III 400 MHz, Bruker, Fällanden, Switzerland).

### 3. Results and Discussion

#### 3.1. Characterization of the palladium encapsulated CPVC nanofibers

$\text{PdCl}_2/\text{CPVC}$  mixture solution was readily electrospun into uniform composite nanofibers due to the excellent spinnability of CPVC (Fig. 1a). The abundant C-Cl groups in CPVC molecules provided the sites for chemical modification and crosslinking by nucleophilic reagents, so the CPVC can react with ethylenediamine to form crosslinked spatial net configuration to improve the solvent resistance of CPVC nanofibers. In addition, the amino groups inside the nanofibers after crosslinking can provide the chelating sites for palladium nanoparticles. As shown in Fig. 1b, the composite nanofibers become thicker after reacting with ethylenediamine. Fig. 1c shows

that the Pd@ACPVC was insoluble in THF, indicating that the CPVC molecules in Pd@ACPVC nanofibers had been sufficiently crosslinked by ethylenediamine.

---Fig. 1---

The reaction of CPVC with ethylenediamine was first analyzed by FT-IR spectra (Fig. 2). The new absorption peaks at  $3275\text{ cm}^{-1}$  and  $1540\text{ cm}^{-1}$  were attributed to the stretching and deformation vibration of amino groups, indicating that the CPVC molecules had been reacted with ethylenediamine. Due to the elimination of HCl from CPVC, a new peak at  $1662\text{ cm}^{-1}$  corresponding to  $\text{-C=C-}$  groups was found [26]. In addition, the new absorption peak at  $1086\text{ cm}^{-1}$  (due to C-O group) demonstrates the partially hydrolysis of C-Cl bond in CPVC molecules. After encapsulation of palladium nanoparticles, the absorption peak assigned to amino groups was blue shifted to  $1563\text{ cm}^{-1}$  from  $1540\text{ cm}^{-1}$ , indicating the coordination of amino groups with palladium nanoparticles. Besides FT-IR spectra, XPS characterization shows that the amination process raised the palladium electron binding energies ( $3d_{5/2}$  and  $3d_{3/2}$ ) separately from  $337.68\text{ eV}$  to  $337.98\text{ eV}$  and  $342.88\text{ eV}$  to  $343.28\text{ eV}$ , which evidently indicated the coordination of palladium with amino groups (Fig. 3). The reduction of  $\text{Pd}^{2+}$  cations into  $\text{Pd}^0$  species was confirmed by decrement of palladium electron binding energies. In addition, the elemental analysis result shows that the nitrogen content in the Pd@ACPVC were  $6.843 \pm 0.502\%$ , indicating that the CPVC molecules had been successfully reacted with ethylenediamine.

---Fig. 2---, --Fig. 3---

Because temperature is an important factor for the palladium catalyzed reactions, the thermal stability of supporting matrices is critical for application of supported palladium catalysts. As shown in Fig. 4, the weight loss at temperature below  $150\text{ }^{\circ}\text{C}$  was ascribed to the

loss of physically absorbed water. The crosslinking of CPVC molecules made the decomposition temperature of nanofibers increased to 236 °C from 176 °C. Thus, the thermal stability of Pd@ACPVC could satisfy the high reaction temperature in the following catalysis reactions.

---Fig. 4---

SEM-EDS analysis shows that the palladium species were homogeneously dispersed in the Pd@ACPVC nanofibers (Fig. 5). In addition, nitrogen and oxygen elements were also found in the fiber, which confirmed the amination and hydrolysis of CPVC molecules. Moreover, the XRD pattern of Pd@ACPVC before reduction had only one intense peak at  $2\theta = 23^\circ$ , which was ascribed to crystal phase of CPVC polymer (Fig. 6a) [32]. After reduction, a new weak peak at  $2\theta = 40^\circ$  assigned to (111) plane of face centered cubic (FCC) Pd<sup>0</sup> crystal appeared [33]. This result also demonstrates that the reducing agent had diffused into the nanofiber to reduce Pd<sup>2+</sup> cations into Pd<sup>0</sup> nanoparticles. In addition, TEM image shows that the palladium nanoparticles with mean diameter of ~3.13 nm dispersed homogeneously inside the nanofibers (Fig. 6b). Thus, we believed that the reactants can also migrate inside the nanofiber to the palladium species to complete the catalysis reaction.

----Fig. 5---, ---Fig. 6---

### 3.2. Heck reaction

Heck reaction is a powerful method for the construction of sp<sup>2</sup>-sp<sup>2</sup> carbon-carbon bonds in the synthesis of various fine chemicals and pharmaceutically active compounds [34,35]. Herein, Heck reaction was employed as a model reaction to evaluate the catalytic performance of Pd@ACPVC. As shown in Fig. 7, increments of reaction temperature and catalyst loading can promote Pd@ACPVC catalyzed Heck reaction of iodobenzene with *n*-butyl acrylate. The Heck

reaction could be carried out with satisfied yields at temperature of 110 °C and Pd@ACPVC loading of 0.221 mol%, which were used in the catalysis reaction afterward. Interestingly, this Pd@ACPVC catalyst had similar catalytic activity with the palladium nanoparticles deposited on functionalized CPVC nanofibers [30,31]. Thus, it can be concluded that encapsulation of palladium nanoparticles inside the ACPVC nanofibers have no obviously negative effect on the catalytic activity, which can be ascribed to the ultrafine fiber.

---Fig. 7---

The Pd@ACPVC catalysis protocol was used to catalyze the Heck reaction with additional aromatic halides with alkenes, and the related results were summarized in Table 1. Examination 1-7 in Table 1 shows that the Pd@ACPVC was very active to catalyze the Heck reaction of aromatic iodides with *n*-butyl acrylate to synthesize the products in moderate to excellent yields. Besides the *n*-butyl acrylate, the Pd@ACPVC can also effectively catalyze the Heck reaction of iodobenzene with other two alkenes (Entry 8 and 9 in Table 1). Unfortunately, the catalytic activity of Pd@ACPVC was comparably low for the Heck reactions of aromatic bromides with *n*-butyl acrylate, which could be attributed to the greater bond strength of carbon-bromine bond (Entry 10-12 in Table 1). As many palladium nanoparticles deposited on polymer solid matrices were also not very active to catalyze the Heck reactions of aromatic bromides, the encapsulation of palladium nanoparticles inside nanofibers was not the reason responsibility for the low catalytic activity of Pd@ACPVC for Heck reactions of aromatic bromides [36,37].

---Table 1---

### 3.3. Sonogashira reaction

Sonogashira reaction is the cross-coupling reaction of aromatic halides with terminal alkynes,

which provides a powerful and versatile method for the construction of  $sp^2$ - $sp$  carbon-carbon bonds [38,39]. Herein, the catalytic activity of Pd@ACPVC was also examined for Sonogashira reactions. Fig. 8 clearly shows that excellent coupling yield of iodobenzene with phenyl acetylene was achieved with Pd@ACPVC loading of 0.133 mol%.

---Fig. 8---

Then, the Pd@ACPVC has been examined for Sonogashira reactions of phenyl acetylene with several additional representative aromatic halides. Examination of entry 1-7 in Table 2 shows that the Pd@ACPVC can effectively catalyze the Sonogashira reactions of aromatic iodides with phenyl acetylene to afford the products with satisfied yields (84-98%). In addition, the aromatic iodides with electron-deficient groups were more active than these with electron-rich groups. Moreover, examination of entry 8-10 in Table 2 shows that the Pd@ACPVC was also efficient to catalyze the Sonogashira reactions of iodobenzene with different aromatic alkynes with satisfied yields (81-92%). Unfortunately, the catalytic activity of Pd@ACPVC was also relatively low for the aromatic bromides (Entry 7 and 8 in Table 2).

---Table 2---

### 3.4. Reuse of the Pd@ACPVC catalyst

The easy separation, recovery and reuse were the fascinating characteristics of heterogeneous palladium catalysts. Due to the regular structure, the fiber catalyst can be readily separated and recovered by simple filtration for reuse. The Heck reaction of iodobenzene with *n*-butyl acrylate and Sonogashira reaction of iodobenzene with phenyl acetylene were again employed to assess the reusability of Pd@ACPVC. Fig. 9 shows that the Pd@ACPVC could be separately reused 10 times for Heck reaction and 6 times for Sonogashira reaction without significant decrement of

coupling yields. Compared with palladium nanoparticles deposited on ACPVC nanofibers [30,31], the reusability of Pd@ACPVC catalyst was significantly improved. Thus, encapsulation of palladium nanoparticles inside the nanofibers can indeed improve its stability and reusability.

---Fig. 9---

Because the palladium aggregation and leaching were the two main reasons responsible for the loss of catalytic activity, the palladium content and dispersion of the recovered Pd@ACPVC catalyst were analyzed by ICP-AES and SEM-EDS (Fig. 10). The palladium contents of the recovered Pd@ACPVC catalyst determined by ICP-AES and SEM-EDS were 0.48% and 0.35% (For Heck reaction), indicating that the palladium leaching was not significant. In addition, SEM-EDS analysis shows that the palladium species were still dispersed evenly in the Pd@ACPVC nanofibers. Moreover, compared with the fresh Pd@ACPVC catalyst, the nitrogen content was decreased while the oxygen content was increased, which could be ascribed to the degradation of ACPVC matrix. In addition, FT-IR analysis of the recovered Pd@ACPVC shows that a new peak at  $1726\text{ cm}^{-1}$  attributed to C=O groups appeared, which also confirmed the degradation of polymer matrix (Fig. 2). Interestingly, the fibrous structure of Pd@ACPVC was still well retained even after 10 cycles (Fig. 11), which could be ascribed to the excellent mechanical property of CPVC polymer. Thus, it can be concluded that the chelating groups (amino groups) were partially lost in the catalysis procedure due to the degradation of polymer matrix, which would weaken the interaction between palladium nanoparticles with ACPVC polymer matrix.

---Fig. 10---, ---Fig. 11---

### 3.5. Comparison of Catalysts

In order to evaluate the catalytic performance of the Pd@ACPVC catalyst, some reported supported palladium catalysts for the Heck reaction of iodobenzene with alkene were summarized in Table 3. The Pd@ACPVC has comparable or better catalytic activity and stability for the Heck reaction. In addition, the recovery and reuse of this fibrous Pd@ACPVC catalyst are quicker and easier than those of the other particulate catalysts.

---Table 3---

### 3.6. Characterization of internal structure of composite nanofibers

As the palladium nanoparticles were encapsulated inside the nanofiber, the internal structure of composite nanofibers not only restricted the leaching and aggregation of palladium nanoparticles, but also allowed the diffusion of reactants and products. Herein, PALS was employed to analyze the inner structure of nanofibers. It is well known that PALS was a sensitive method to assess the size and concentration of the free volume holes of condensed materials [45-47]. The PALS spectra can be resolved into three components ( $\tau_1$ ,  $\tau_2$  and  $\tau_3$ ) and the long lived component  $\tau_3$  is signed to the *o*-Ps pick-off annihilation in free volume holes in amorphous regions of polymeric materials. Thus, the radius of free volume holes (R) can be calculated based on the following equation (Equation 1) [45-47]:

$$\frac{1}{\tau_3} = 2 \left[ 1 - \frac{R}{R + 0.1656} + \frac{1}{2\pi} \text{Sin} \left( \frac{2\pi R}{R + 0.1656} \right) \right] \quad \text{Equation 1}$$

As the crosslinking restricts the movement of CPVC molecules in composite nanofibers, the free volume size decreased after crosslinking reaction (Table 4). After reuse, the size of free volume holes was increased while the corresponding concentration was reduced, which could be

ascribed to degradation of ACPVC polymeric matrix. The CPVC polymer could be degraded under high temperature due to the dehydrochlorination and oxidation reactions [48,49]. As a result, the capping effect of palladium nanoparticles by the crosslinked CPVC molecules was also weakened, resulting in the aggregation and leaching of palladium nanoparticles.

---Table 4---

#### 4. Conclusions

In summary, we have prepared uniform Pd<sup>2+</sup>/CPVC composite nanofibers by electrospinning. Then, the CPVC molecules inside the nanofibers were readily functionalized and crosslinked by ethylenediamine. These composite nanofibers have exhibited high catalytic activity and stability for Heck and Sonogashira reactions of aromatic iodides, which can be attributed to the chelating ability of amino groups on polymeric chain, encapsulation of palladium nanoparticles inside the nanofibers and ultrafine fiber. The reuse of these composite nanofibers would lead to the loss of functional groups (amino groups) and expansion of free volume holes, resulting in the leaching of palladium nanoparticles. The high catalytic activity and easy operation make this unique environmentally benign heterogeneous palladium catalyst to be attractive for large industrial-scale applications.

#### Acknowledgement

The authors acknowledge the financial support from the National Natural Science Foundation of China (No. 11905132 and 11975157).

**References**

- [1] J. Tsuji, *Palladium Reagents and Catalysts: New Perspectives for 21<sup>st</sup> century*, John Wiley & Sons, 2004.
- [2] A. Del Zotto, D. Zuccaccia, Metallic palladium, PdO, and palladium supported on metal oxides for the Suzuki–Miyaura cross-coupling reaction: a unified view of the process of formation of the catalytically active species in solution. *Catal. Sci. Technol.* 7 (2017) 3934-3951.
- [3] T. Glasnov, S. Findenig, C. Kappe, Heterogeneous versus homogeneous palladium catalysts for ligandless Mizoroki–Heck reactions: A comparison of batch/microwave and continuous - flow processing, *Chem. - Eur. J.* 15 (2009) 1001-1010.
- [4] H. Veisi, T. Tamoradi, B. Karmakar, S. Hemmati, Green tea extract-modified silica gel decorated with palladium nanoparticles as a heterogeneous and recyclable nanocatalyst for Buchwald-Hartwig C-N crosscoupling reactions. *J. Phys. Chem. Solids* 138 (2020) 109256.
- [5] X. Liu, W. Xu, D. Xiang, Z. Zhang, H. Lin, Palladium immobilized on functionalized hypercrosslinked polymers: a highly active and recyclable catalyst for Suzuki-Miyaura coupling reactions in water. *New J. Chem.* 43 (2019) 12206-12210.
- [6] M. Nasrollahzadeh, N. Motahharifar, F. Ghorbannezhad, N.S.S. Bidgoli, T. Baran, R.S. Varma, Recent advances in polymer supported palladium complexes as (nano)catalysts for Sonogashira coupling reaction. *Mol. Catal.* 480 (2020) e110645.
- [7] H. Veisi, T. Ozturk, B. Karmakar, T. Tamoradi, S. Hemmati, In situ decorated Pd NPs on chitosan-encapsulated Fe<sub>3</sub>O<sub>4</sub>/SiO<sub>2</sub>-NH<sub>2</sub> as magnetic catalyst in Suzuki-Miyaura coupling and 4-nitrophenol reduction. *Carbohydr. Polym.* 235 (2020) 115966.

- [8] T. Tamoradi, H. Veisi, B. Karmakar, Pd Nanoparticle fabricated tetrahydroharman-3-carboxylic acid analog immobilized  $\text{CoFe}_2\text{O}_4$  catalyzed fast and expedient C-C cross and C-S coupling. *ChemistrySelect* 4 (2019) 10953-10959.
- [9] H. Veisi, T. Tamoradi, B. Karmakar, P. Mohammadi, S. Hemmati, In situ biogenic synthesis of Pd nanoparticles over reduced graphene oxide by using a plant extract (*Thymbra spicata*) and its catalytic evaluation towards cyanation of aryl halides. *Mat. Sci. Eng. C* 104 (2019) 109919.
- [10] Y. Rangraz, F. Nemati, A. Elhampour, A novel magnetically recoverable palladium nanocatalyst containing organoselenium ligand for the synthesis of biaryls via Suzuki-Miyaura coupling reaction. *J. Phys. Chem. Solids* 138 (2020) 109251.
- [11] S.K. Dey, D. Dietrich, S. Wegner, B. Gil-Hernández, C. Janiak, Palladium nanoparticle-immobilized porous polyurethane material for quick and efficient heterogeneous catalysis of Suzuki-Miyaura cross-coupling reaction at room temperature. *Chemistryselect* 3 (2018) 1365-1370.
- [12] A.R. Hajipour, F. Mohammadsaleh, Triazole-functionalized silica supported palladium(II) complex: a novel and highly active heterogeneous nano-catalyst for C-C coupling reactions in aqueous media. *Catal. Lett.* 148 (2018) 1035-1046.
- [13] L. Shao, J. Liu, Y. Ye, Zhang X.M., Qi C, Polyacrylonitrile fiber mat-supported palladium catalyst for Mizoroki-Heck reaction in aqueous solution. *Appl. Organomet. Chem.* 25 (2011) 699-703.
- [14] G.Z. Fan, S.Q. Cheng, M.F. Zhu, X.L. Gao, Palladium chloride anchored on organic functionalized MCM-41 as a catalyst for the Heck reaction. *Appl. Organomet. Chem.* 21 (2007) 670-675.

- [15] Pooja, P.B. Barman, S.K. Hazra, Role of capping agent in palladium nanoparticle based hydrogen sensor. *J. Clust. Sci.* 29 (2018) 1209-1216.
- [16] M. Farrag, R.A. Mohamed, Ecotoxicity of ~1 nm silver and palladium nanoclusters protected by l-glutathione on the microbial growth under light and dark conditions. *J. Photoch. Photobio. A: Chem.* 330 (2016) 117-125.
- [17] R. Khatun, P. Bhanja, P. Mondal, A. Bhaumik, D. Das, S. ManirulIslam, Palladium nanoparticles embedded over mesoporous TiO<sub>2</sub> for chemical fixation of CO<sub>2</sub> under atmospheric pressure and solvent-free conditions. *New J. Chem.* 41 (2017) 12937-12946.
- [18] S. Xu, M. Wang, B. Feng, X. Han, Z. Lan, H. Gu, H. Li, H. Li, Dynamic kinetic resolution of amines by using palladium nanoparticles confined inside the cages of amine-modified MIL-101 and lipase. *J. Catal.* 363 (2018) 9-17.
- [19] C. Zhang, R. Zhang, S. He, L. Li, X. Wang, M. Liu, W. Chen, 4-Nitrophenol reduction by a single platinum palladium nanocube caged within a nitrogen-doped hollow carbon nanosphere. *Chemcatchem* 9 (2016) 980-986.
- [20] M.M. Demir, M.A. Gulgun, Y.Z. Menciloglu, B. Erman, S.S. Abramchuk, E.E. Makhaeva, A.R. Khokhlov, V.G. Matveeva, M.G. Sulman, Palladium nanoparticles by electrospinning from poly(acrylonitrile-co-acrylic acid)-PdCl<sub>2</sub> solutions. Relations between preparation conditions, particle size, and catalytic activity. *Macromolecules* 37 (2004) 1787-1792.
- [21] S.J. Park, S. Bhargava, E.T. Bender, G.G. Chase, R.D.J. Ramsier, Palladium nanoparticles supported by alumina nanofibers synthesized by electrospinning *J. Mater. Res.* 23 (2008) 1193-1196.

- [22] L. Guo, J. Bai, H. Liang, T. Xu, C. Li, Q. Meng, H. Liu, Y. Huang, A facile approach to preparing palladium nanoparticles-embedded polyvinylpyrrolidone (PVP) heterogeneous hybrid nanofibers mats by electrospinning. *Korean J. Chem. Eng.* 30 (2013) 2142-2150.
- [23] B. Yu, Y. Liu, G. Jiang, D. Liu, W. Yu, H. Chen, L. Li, Preparation of electrospun Ag/g-C<sub>3</sub>N<sub>4</sub> loaded composite carbon nanofibers for catalytic applications. *Mater. Res. Express* 4 (2017) 15603.
- [24] J.Y. Cheon, Y.O. Kang, W.H. Park, Formation of Ag nanoparticles in PVA solution and catalytic activity of their electrospun PVA nanofibers. *Fiber. Polym.* 16 (2015) 840-849.
- [25] T. Baran, N.Y. Baran, A. Menteş, An easily recoverable and highly reproducible agar-supported palladium catalyst for Suzuki-Miyaura coupling reactions and reduction of o-nitroaniline. *Int. J. Boil. Macromol.* 115 (2018) 249-256.
- [26] D. Wang, C. Bao, Q. Luo, R. Yin, X. Li, J. An, Z. Xu, Improved visible-light photocatalytic activity and anti-photocorrosion of Cds nanoparticles surface-modified by conjugated derivatives from polyvinyl chloride. *J. Environ. Chem. Eng.* 3 (2015) 1578-1585.
- [27] L. Zhang, M. Xue, Y. Cui, Catalytic performance of PVC-triethylene-tetramine supported palladium complex for Heck reaction. *J. Appl. Polym. Sci.* 115 (2010) 2523-2527.
- [28] M. Samarasimhareddy, G. Prabhu, T.M. Vishwanatha, V.V. Vommina. PVC-supported palladium nanoparticles: An efficient catalyst for Suzuki cross-coupling reactions at room temperature. *Synthesis* 45 (2013) 1201-1206.
- [29] H.P. Hemantha, S.V. Sureshbahu, Poly(vinyl)chloride supported palladium nanoparticles: catalyst for rapid hydrogenation reactions. *Org. Biomol. Chem.* 9 (2011) 2597-2601.

- [30] L. Shao, C. Qi, X.M. Zhang. Aminated chlorinated polyvinylchloride nanofiber mat-supported palladium heterogeneous catalysts: preparation, characterization and applications. *RSC Adv.* 4 (2014) 53105-53108.
- [31] L. Shao, L. Lian, C. Qi, Novel palladium catalysts immobilized on functionalized chlorinated polyvinylchloride nanofiber mats. *Kinet. Catal.* 58 (2017) 370-376.
- [32] S.A. Nouh, A. Abou Elfadl, B.O. Alsobhi, A.M. Massoud, Optical, structure and thermal investigation of the effect of gamma radiation in CPVC/Ag and CPVC/Pd nanocomposites membrane. *Radiat. Eff. Defect. S.* 174 (2019) 111-124.
- [33] H. Veisi, S.A. Mirshokraie, H. Ahmadian, Synthesis of biaryls using palladium nanoparticles immobilized on metformine-functionalized polystyrene resin as a reusable and efficient nanocatalyst. *Int. J. Biol. Macromol.* 108 (2018) 419-425.
- [34] A.R. Hajipour, A.R. Sadeghi, Z. Khorsandi, Pd nanoparticles immobilized on magnetic chitosan as a novel reusable catalyst for green Heck and Suzuki cross - coupling reaction: in water at room temperature. *Appl. Organomet. Chem.* 32 (2018) e4112.
- [35] T. Baran, N.Y. Baran, A. Menteş, An easily recoverable and highly reproducible agar-supported palladium catalyst for Suzuki-Miyaura coupling reactions and reduction of o-nitroaniline. *Int. J. Biol. Macromol.* 115 (2018) 249-256.
- [36] L. Nie, L. Liang, M. Jiang, L. Shao, C. Qi, In situ cross-linked chitosan composite superfine fiber via electrospinning and thermal treatment for supporting palladium catalyst. *Fiber. Polym.* 19 (2018) 1463-1471.
- [37] K. Zhan, H. You, W. Liu, J. Lu, P. Lu, J. Dong, Pd nanoparticles encaged in nanoporous

interpenetrating polymer networks: A robust recyclable catalyst for Heck reactions. *React. Funct. Polym.* 71 (2011) 756-765.

[38] F. Zhu, P. Zhao, Q. Li, D. Yang, Synthesis and characterization of mesoporous Pd(II) organometal nanoplatelet catalyst for copper-free Sonogashira reaction in water. *J. Organomet. Chem.* 859 (2018) 92-98.

[39] M. Dabiri, M.P. Vajargahy, PdCo bimetallic nanoparticles supported on three - dimensional graphene as a highly active catalyst for Sonogashira cross-coupling reaction. *Appl. Organomet. Chem.* 31 (2017) e3594.

[40] Y. Huang, L. Yang, M. Huang, J. Wang, L. Xu, L.W. Li, H. Zhou, X. Sun, H. Xing, H. Liu, Polystyrene microsphere-immobilized palladium(II) porphyrin as mild, reusable, and highly efficient catalyst for Heck reaction. *Particuology* 22 (2015) 128-133.

[41] H. Hagiwara, Y. Shimizu, T. Hoshi, T. Suzuki, M. Ando, K. Ohkubo, C. Yokoyama, Heterogeneous Heck reaction catalyzed by Pd/C in ionic liquid. *Tetrahedron Lett.* 42 (2001) 4349-4351.

[42] K.R. Balinge, P.R. Bhagat, A polymer-supported salen-palladium complex as a heterogeneous catalyst for the Mizoroki-Heck cross-coupling reaction. *Inorg. Chim. Acta* 495 (2019) 119017.

[43] S. Asadbegi, M.A. Bodaghifard, E. Alimohammadi, R.Ahangarani-Farahani, Immobilization of palladium on modified nanoparticles and its catalytic properties on Mizoroki-Heck reaction. *ChemistrySelect* 3 (2018) 13297-13302.

[44] G. Xing, Palladium immobilized on aminated polyacrylonitrile nanofiber as an efficient

heterogeneous catalyst for Heck reaction. *Fiber. Polym.* 17 (2016) 194-198.

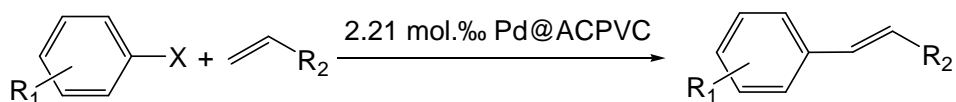
[45] S.J. Tao, Positronium annihilation in molecular substances. *J. Chem. Phys.* 56 (1972) 5499-5510.

[46] S. Khoonsap, S. Rugmai, W.S. Hung, K.R. Lee, S. Amnuaypanich, Promoting permeability-selectivity anti-trade-off behavior in polyvinyl alcohol (PVA) nanocomposite membranes. *J. Membr. Sci.* 544 (2017) 287-296.

[47] E. Lizundia, I. Serna, E. Axpe, J.L. Vilas, Free-volume effects on the thermomechanical performance of epoxy-SiO<sub>2</sub> nanocomposites. *J. Appl. Polym. Sci.* 134 (2017) 45216.

[48] E.O. Elakesh, T.R. Hull, D. Price, P. Carty, Effect of stabilisers and lubricant on the thermal decomposition of chlorinated poly(vinyl chloride) (CPVC). *Polym. Degrad. Stabil.* 88 (2005) 41-45.

[49] E.O. Elakesh, T.R. Hull, D. Prcie, P. Carty, Thermal decomposition of chlorinated poly(vinyl chloride) (CPVC). *J. Vinyl Additi. Techn.* 9 (2003) 116-126.

**Table 1.** Pd@ACPVC catalyzed Heck reaction of aromatic halides with alkenes.<sup>a</sup>

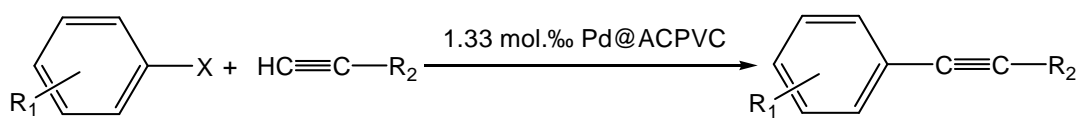
| Entry | R <sub>1</sub>      | X   | R <sub>2</sub>                                      | Time (h) | Yield (%) <sup>b</sup> |
|-------|---------------------|-----|---|----------|------------------------|
| 1     | 2-F-                | I-  | -COO(CH <sub>2</sub> ) <sub>3</sub> CH <sub>3</sub> | 5        | 77                     |
|       |                     |     |   | 10       | 90                     |
| 2     | 4-F-                | I-  | -COO(CH <sub>2</sub> ) <sub>3</sub> CH <sub>3</sub> | 5        | 85                     |
|       |                     |     |   | 10       | 97                     |
| 3     | 2-Br-               | I-  | -COO(CH <sub>2</sub> ) <sub>3</sub> CH <sub>3</sub> | 5        | 57                     |
|       |                     |     |   | 10       | 87                     |
| 4     | 4-Cl-               | I-  | -COO(CH <sub>2</sub> ) <sub>3</sub> CH <sub>3</sub> | 5        | 44                     |
|       |                     |     |   | 10       | 94                     |
| 5     | 2-CH <sub>3</sub> - | I-  | -COO(CH <sub>2</sub> ) <sub>3</sub> CH <sub>3</sub> | 5        | 31                     |
|       |                     |     |   | 10       | 90                     |
| 6     | 3-CH <sub>3</sub> - | I-  | -COO(CH <sub>2</sub> ) <sub>3</sub> CH <sub>3</sub> | 5        | 43                     |
|       |                     |     |   | 10       | 92                     |
| 7     | 4-CH <sub>3</sub> - | I-  | -COO(CH <sub>2</sub> ) <sub>3</sub> CH <sub>3</sub> | 5        | 19                     |
|       |                     |     |   | 10       | 81                     |
| 8     | H-                  | I-  | -COO(CH <sub>2</sub> ) <sub>3</sub> CH <sub>3</sub> | 5        | 98                     |
| 8     | H-                  | I-  | -COOCH <sub>3</sub>                                 | 5        | 74                     |
|       |                     |     |   | 10       | 98                     |
| 9     | H-                  | I-  | -Ph <sup>c</sup>                                    | 5        | 43                     |
|       |                     |     |   | 24       | 84                     |
| 10    | H-                  | Br- | -COO(CH <sub>2</sub> ) <sub>3</sub> CH <sub>3</sub> | 5        | 10                     |
|       |                     |     |   | 24       | 52                     |
| 11    | 4-F-                | Br- | -COO(CH <sub>2</sub> ) <sub>3</sub> CH <sub>3</sub> | 5        | 15                     |
|       |                     |     |   | 24       | 77                     |

|    |                     |     |   |    |    |
|----|---------------------|-----|---|----|----|
| 12 | 4-NO <sub>2</sub> - | Br- | -COO(CH <sub>2</sub> ) <sub>3</sub> CH <sub>3</sub> | 5  | 19 |
|    |                     |     |   | 24 | 61 |

<sup>a</sup>: Reaction condition: aromatic halide: 1.0 mmol; alkene: 2.0 mmol; triethylamine: 2.5 mmol; Pd@ACPVC: 25 mg (0.221 mol%); glycol: 0.2 g; DMAc: 3.2 mL; Reaction temperature: 110 °C (for aromatic iodides) or 130 °C (for aromatic bromides).

<sup>b</sup>: Product yields, based on the amount of aromatic iodides, were determined from GC/MS measurements.

<sup>c</sup>: Phenyl group.

**Table 2.** Pd@ACPVC catalyzed Sonogashira reaction of aromatic halides with alkynes.<sup>a</sup>


| Entry | R <sub>1</sub>    | X  | R <sub>2</sub> <sup>c</sup> | Time (h) | Yield (%) <sup>b</sup> |
|-------|-------------------|----|-----------------------------|----------|------------------------|
| 1     | 2-F               | I  | Ph                          | 5        | 49                     |
|       |                   |    |                             | 10       | 89                     |
| 2     | 4-F               | I  | Ph                          | 5        | 45                     |
|       |                   |    |                             | 24       | 95                     |
| 3     | 2-Br              | I  | Ph                          | 5        | 36                     |
|       |                   |    |                             | 24       | 88                     |
| 4     | 2-Cl              | I  | Ph                          | 5        | 28                     |
|       |                   |    |                             | 24       | 91                     |
| 5     | 2-CH <sub>3</sub> | I  | Ph                          | 5        | 37                     |
|       |                   |    |                             | 24       | 86                     |
| 6     | 4-CH <sub>3</sub> | I  | Ph                          | 5        | 21                     |
|       |                   |    |                             | 24       | 84                     |
| 7     | H                 | I  | Ph                          | 5        | 98                     |
| 8     | H                 | I  | 4-F-Ph                      | 5        | 36                     |
|       |                   |    |                             | 24       | 84                     |
| 9     | H                 | I  | 2-Cl-Ph                     | 5        | 48                     |
|       |                   |    |                             | 24       | 92                     |
| 10    | H                 | I  | 2-Th                        | 5        | 27                     |
|       |                   |    |                             | 24       | 81                     |
| 11    | H                 | Br | Ph                          | 5        | 16                     |
|       |                   |    |                             | 24       | 33                     |
| 12    | 4-F               | Br | Ph                          | 5        | 25                     |

<sup>a</sup>: Reaction condition: aromatic halide: 1.0 mmol; alkyne: 2.0 mmol; K<sub>2</sub>CO<sub>3</sub>: 3.0 mmol; Pd@ACPVC: 15 mg (0.133 mol.%); CuI: 0.02 mmol; glycol: 0.2 g; DMAc: 3.2 mL; 110 °C (for aromatic iodides) or 130 °C (for aromatic bromides).

<sup>b</sup>: Product yields, based on the amount of aromatic halides, were determined from GC/MS measurements.

<sup>c</sup>: Ph: phenyl; Th: 2-thienyl.

**Table 3.** Comparison of catalytic activities of Pd@ACPVC with other supported palladium catalysts.

| Entry | catalyst             | Reaction condition                                     | Yields at the first and last run (%)          |
|-------|----------------------|--|---|
| 1     | Pd@ACPVC (this work) | Pd 0.133 mol%, 110 °C for 3 h, air atmosphere          | 1 <sup>th</sup> : 97%; 10 <sup>th</sup> : 91% |
| 2     | Pd-MTP/PMs [40]      | Pd 0.1 mol%, 100 °C for 4 h, N <sub>2</sub> atmosphere | 1 <sup>th</sup> : 99%; 6 <sup>th</sup> : 98%  |
| 3     | Pd/C [41]            | Pd 10 mol%, 100 °C for 12 h, N <sub>2</sub> atmosphere | 1 <sup>th</sup> : 92%; 6 <sup>th</sup> : 80%  |
| 4     | PS-Pd-Salen [42]     | Pd 0.336 mol%, 110 °C for 10 h, air atmosphere         | 1 <sup>th</sup> : 92%; 5 <sup>th</sup> : 79%  |
| 5     | MNPs-TDAH-Pd [43]    | Pd 5.91 mol%, 100 °C for 8 h, air atmosphere           | 1 <sup>th</sup> : 90%; 5 <sup>th</sup> : 82%  |
| 6     | Pd/PAN fiber [44]    | Pd 2.0 mol%, 110 °C for 3 h, air atmosphere            | 1 <sup>th</sup> : 97%; 4 <sup>th</sup> : 92%  |

**Table 4.** The free volume analyses of composite nanofibers by PALS and corresponding diameters.

| Fiber sample                                | $\tau_3$ (ns)     | $I_3$ (%)         | Diameter of free volume hole (nm) |
|---|-------------------|-------------------|-----------------------------------|
| Pd@CPVC                                     | $2.690 \pm 0.110$ | $2.880 \pm 0.230$ | 0.4304                            |
| Pd@ACPVC                                    | $2.358 \pm 0.021$ | $2.786 \pm 0.032$ | 0.3860                            |
| Pd@ACPVC (after Heck reaction for 10 times) | $2.860 \pm 0.160$ | $1.880 \pm 0.170$ | 0.4511                            |

**Figures Caption**

**Scheme 1.** Schematic representation for the preparation palladium nanoparticles encapsulated aminated CPVC nanofiber (Pd@ACPVC).

**Fig. 1.** SEM images of (a) Pd@CPVC, (b) Pd@ACPVC and (c) Pd@ACPVC after submersing in THF solution for 24 hours.

**Fig. 2.** FT-IR spectra of CPVC, ACPVC, Pd@ACPVC fiber mats before and after catalysis.

**Fig. 3.** X-ray photoelectron spectra (XPS) of Pd@CPVC, Pd@ACPVC fiber mats before and after reduction.

**Fig. 4.** TGA analysis of Pd@CPVC and Pd@ACPVC catalysts.

**Fig. 5.** SEM-EDS analysis of Pd@ACPVC.

**Fig. 6.** (a) XRD patterns and (b) TEM image of Pd@ACPVC.

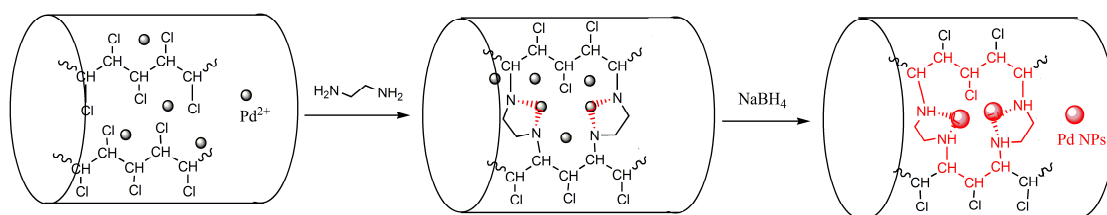
**Fig. 7.** Effects of (a) reaction temperature and (b) catalyst loading on the Pd@ACPVC catalyzed Heck reaction.

**Fig. 8.** Effect of catalyst loading on the Pd@ACPVC catalyzed Sonogashira reaction of iodobenzene with phenyl acetylene.

**Fig. 9.** The reuses of Pd@ACPVC nanofiber mat for (a) Heck reaction of iodobenzene with *n*-butyl acrylate and (b) Sonogashira reaction of iodobenzene with phenyl acetylene.

**Fig. 10.** SEM-EDS analysis of the recovered Pd@ACPVC nanofibers.

**Fig. 11.** SEM image of the recovered Pd@ACPVC.



**Scheme 1.** Schematic representation for the preparation palladium nanoparticles encapsulated aminated CPVC nanofiber (Pd@ACPVC).

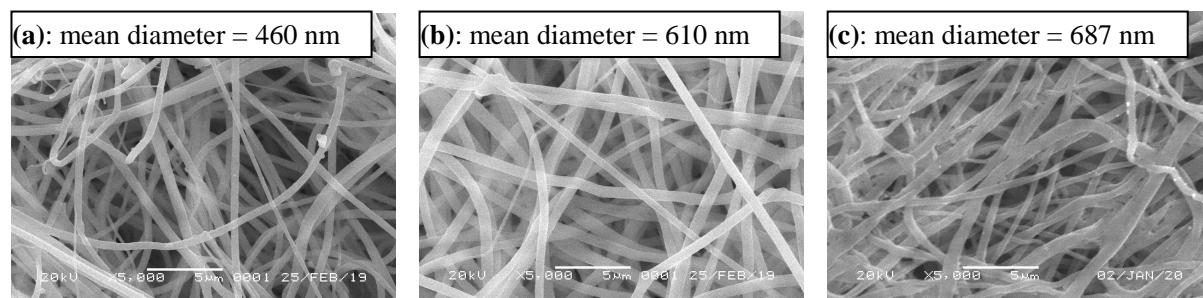


**Fig. 1.** SEM images of (a) Pd@CPVC, (b) Pd@ACPVC and (c) Pd@ACPVC after submersing in THF solution for 24 hours.

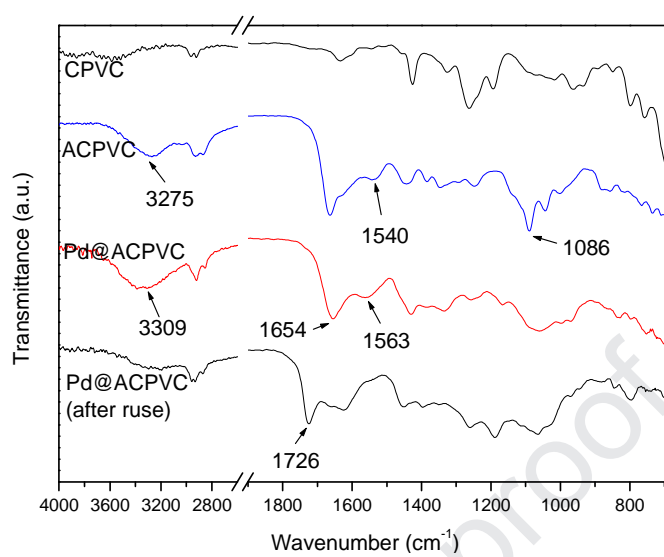


**Fig. 2.** FT-IR spectra of CPVC, ACPVC, Pd@ACPVC fiber mats before and after catalysis.

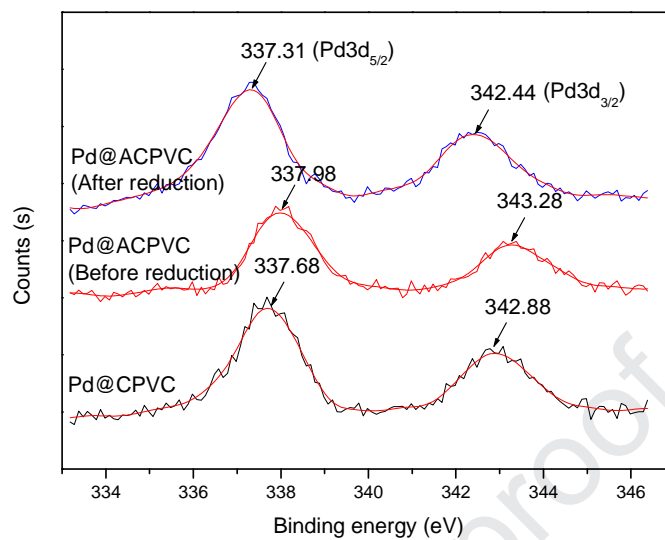


**Fig. 3.** X-ray photoelectron spectra (XPS) of Pd@CPVC, Pd@ACPVC fiber mats before and after reduction.

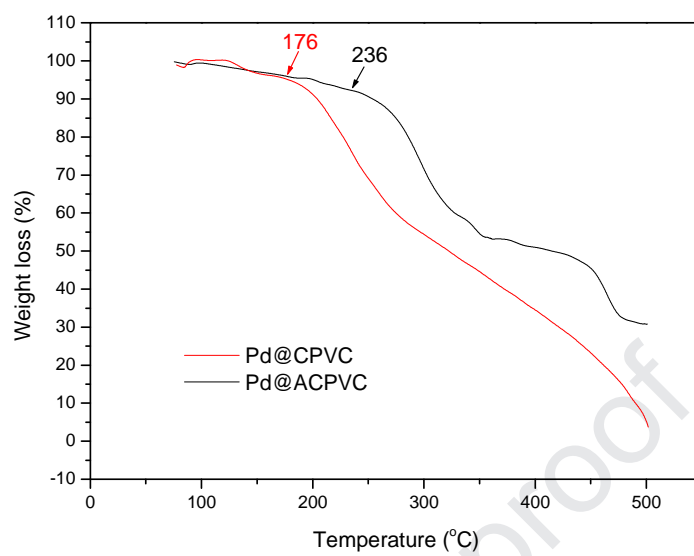


**Fig. 4.** TGA analysis of Pd@CPVC and Pd@ACPVC catalysts.

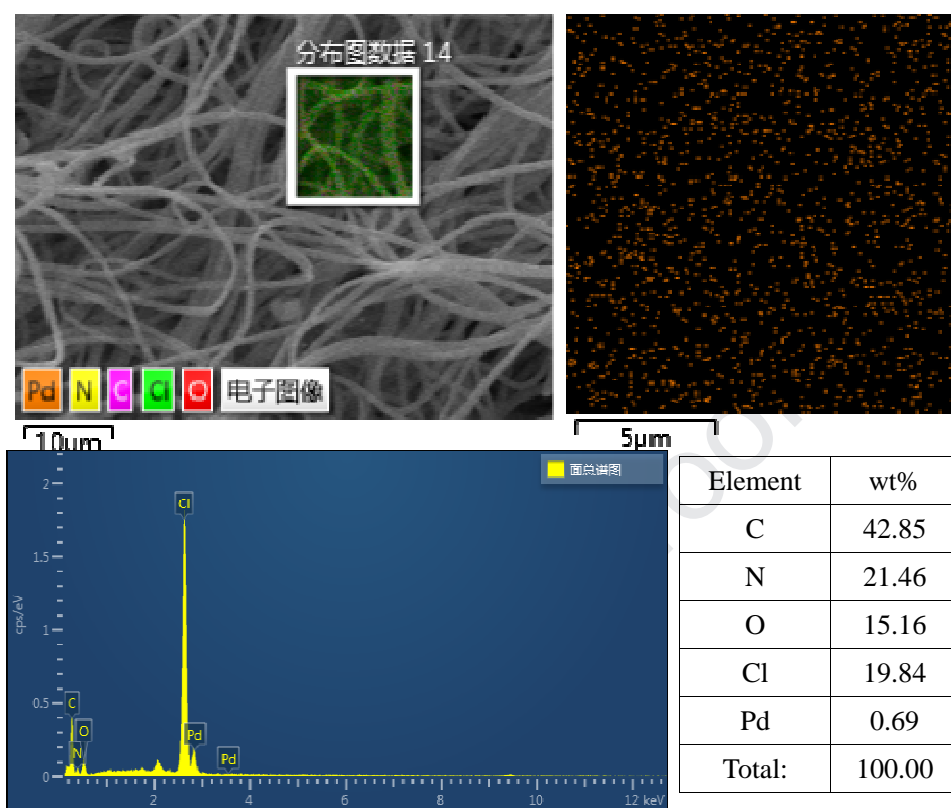


**Fig. 5.** SEM-EDS analysis of Pd@ACPVC.

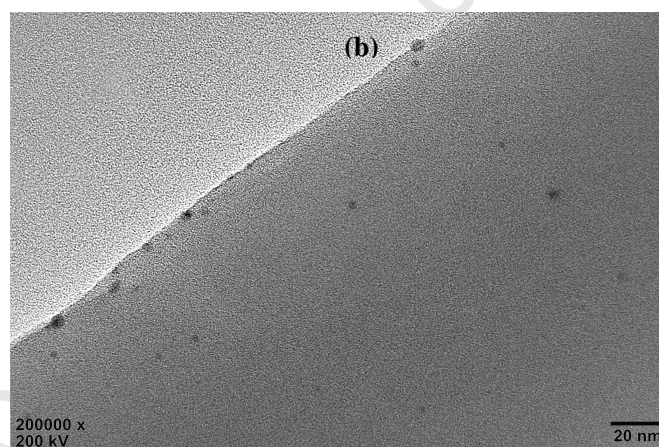
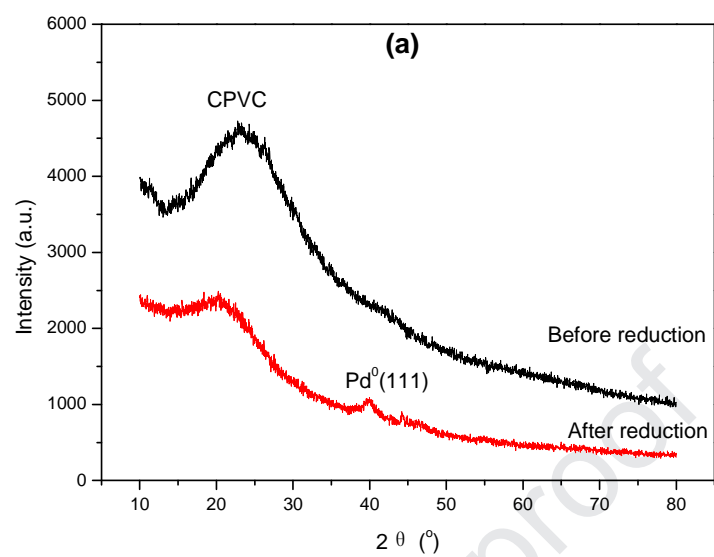


**Fig. 6.** (a) XRD patterns and (b) TEM image of Pd@ACPVC.

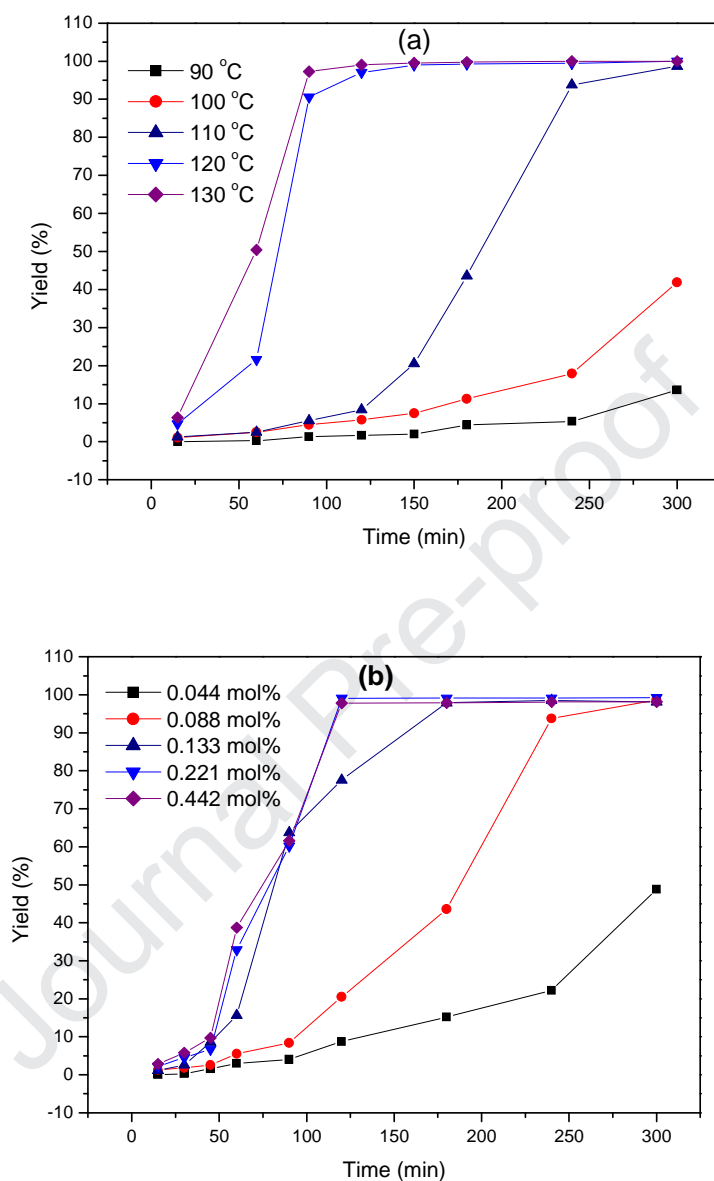


**Fig. 7.** Effects of (a) reaction temperature and (b) catalyst loading on the Pd@ACPVC catalyzed Heck reaction. (Reaction conditions: iodobenzene: 1.0 mmol, *n*-butyl acrylate: 2.0 mmol, triethylamine: 2.5 mmol, glycol: 0.2 g, Pd@ACPVC: 10 mg (0.088 mol%) (a), temperature: 110 °C (b), DMAc: 3.2 mL).

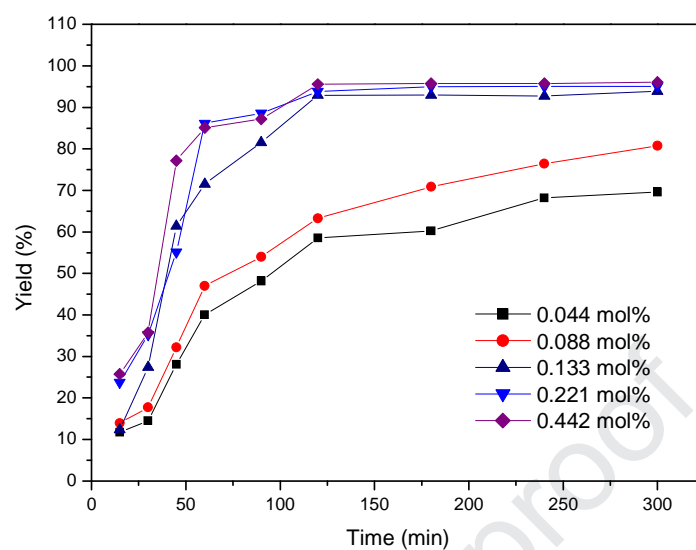


**Fig. 8.** Effect of catalyst loading on the Pd@ACPVC catalyzed Sonogashira reaction of iodobenzene with phenyl acetylene. (Reaction conditions: iodobenzene: 1.0 mmol, phenyl acetylene: 2.0 mmol,  $K_2CO_3$ : 3.0 mmol, CuI: 0.02 mmol, glycol: 0.2 g, DMAc: 3.2 mL, temperature: 110 °C).

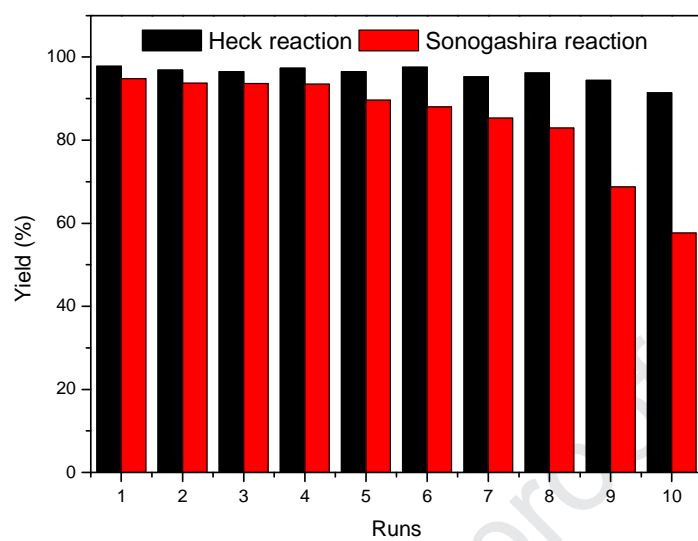


**Fig. 9.** The reuses of Pd@ACPVC nanofiber mat for (a) Heck reaction of iodobenzene with *n*-butyl acrylate and (b) Sonogashira reaction of iodobenzene with phenyl acetylene.

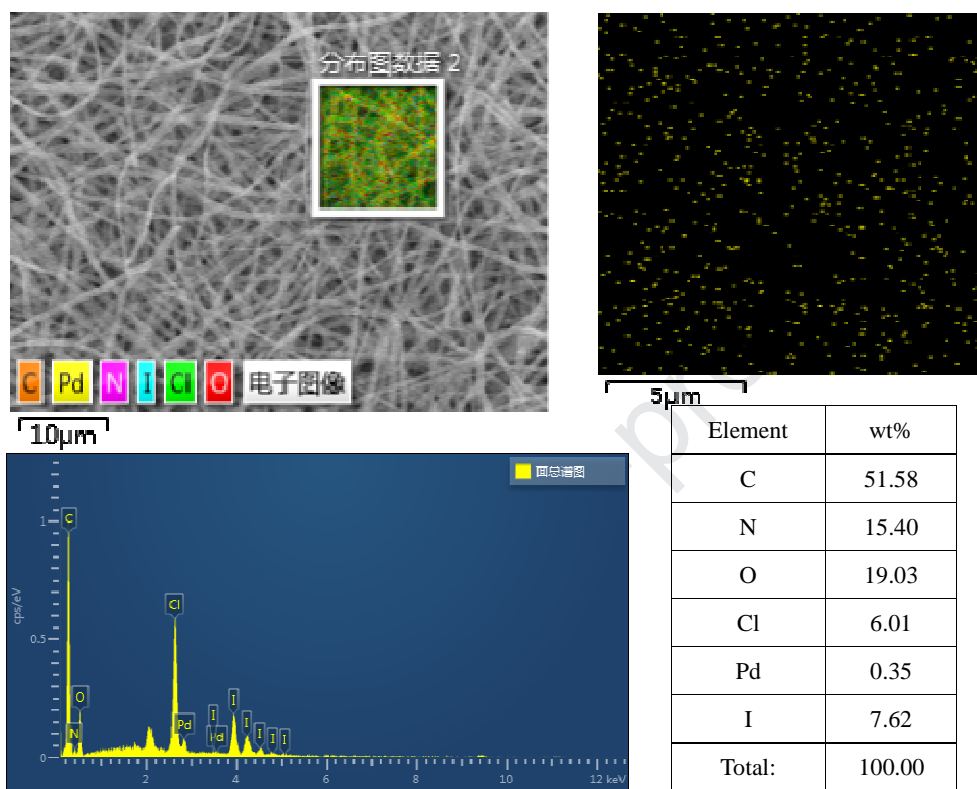


**Fig. 10.** SEM-EDS analysis of the recovered Pd@ACPVC nanofibers.

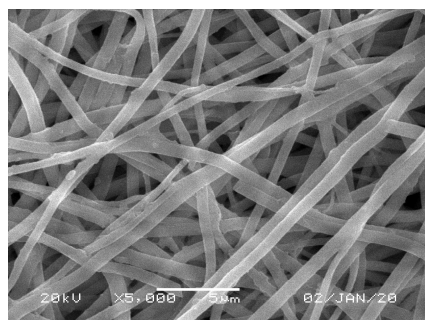


**Fig. 11.** SEM image of the recovered Pd@ACPVC.

### **Highlights**

1. Pd nanoparticles were generated in crosslinked and aminated CPVC nanofibers.
2. Pd nanoparticles were stabilized by chelating and capping effects.
3. These nanofibers exhibited high activity and stability for coupling reactions.
4. The activity decay was resolved by PALS and other common characterizations.

Journal Pre-proof

**Conflict of Interest**

The authors report no conflicts of interest in this work.

Journal Pre-proof